Self-Focusing and Defocusing in Waveguide Arrays

R. Morandotti,* H. S. Eisenberg, and Y. Silberberg
Department of Physics of Complex Systems, Weizmann Institute of Science, Rehovot, Israel 76100

M. Sorel and J. S. Aitchison
Department of Electronics and Electrical Engineering, University of Glasgow, Glasgow, Scotland, G12 8QQ
(Received 21 June 2000)

We show that two regimes of diffraction exist in arrays of waveguides, depending upon the input conditions. At higher powers, normal diffraction leads to self-focusing and to the formation of bright solitons through the nonlinear Kerr effect. By slightly changing the input conditions, light experiences anomalous diffraction and is nonlinearly defocused. For the first time, self-focusing and self-defocusing have been achieved for the same medium, structure, and wavelength.

DOI: 10.1103/PhysRevLett.86.3296 PACS numbers: 42.65.Wi, 42.25.Fx, 42.65.Tg, 42.82.Et

Analogies between dispersion and diffraction are often used in optical science. Although they are two distinct phenomena, they share several common properties. Both lead to the expansion of an initial light profile, the first in time and the second in space. However, while dispersion is material dependent and is absent in vacuum, diffraction is primarily a geometrical phenomenon and it is only slightly affected by the propagation medium through its refractive index.

Depending on the medium, dispersion can be normal or anomalous, while diffraction is always equivalent to anomalous dispersion. This fact has important consequences, particularly to nonlinear propagation. For example, bright and dark temporal solitons have been generated in media with positive Kerr nonlinearities [1–3], while no dark *spatial* solitons have been reported in such media.

The similarities between dispersion and diffraction stem from the way in which different components of light gather optical phase as they propagate. Consider a generic temporal pulse, represented in terms of its spectral frequency components. The phase accumulated by a frequency component ω after propagating a distance L is $k(\omega)L$, where $k(\omega) = 2\pi/\lambda = n(\omega)\omega/c$. Here λ is the wavelength, n is the refractive index, and c is the speed of light in vacuum. A pulse composed of a narrow group of frequencies around ω travels at the group velocity v_g, where $1/v_g = k' = \partial k/\partial\omega$. The distortion and broadening of pulses result from the fact that the group velocity is not uniform for all frequencies composing the pulse. The effect of *group velocity dispersion* (GVD) is related to $k'' = \partial^2 k/\partial\omega^2$ which describes the rate of pulse broadening. We note that when $n(\omega)$ is constant, as in vacuum, no GVD is present ($k'' = 0$). In most optical materials (e.g., glasses in the visible spectrum), dispersion is normal, $k''(\omega) > 0$, while anomalous dispersion, $k''(\omega) < 0$, is obtained at longer wavelengths in the infrared range.

We will now trace, using the considerations above, a parallel between diffraction and dispersion. For simplicity, we will consider a beam which is free to expand (diffract) only along one transverse direction $\hat{x}$. The case of diffraction along two dimensions is a simple extension. Let us consider a cross section of a monochromatic beam along the x axis at $z = 0$. In the same way as a pulse was expressed in terms of its temporal frequencies through Fourier series, the spatial profile of the beam can be decomposed into spatial frequencies k_x, i.e., of plane waves with constant wave number k but different propagation directions. In a homogeneous medium the components of k, k_x and k_z, are related by the condition $k^2 = k_x^2 + k_z^2$ or, equivalently, $k_z = \sqrt{k^2 - k_x^2}$ [Fig. 1(a)].

When an optical field propagates over a distance L, each transverse component of the frequency k_x gains a phase $k_z(k_x) \times L$. The initial profile of the beam along the $\hat{x}$ direction broadens as the beam propagates due to the phase accumulated by the different spatial frequencies. In

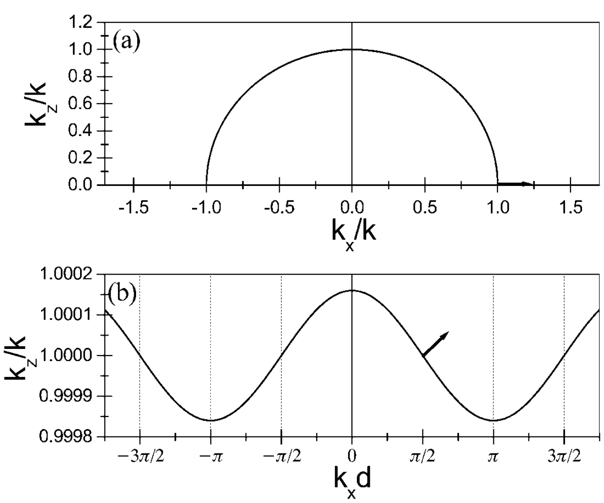

FIG. 1. Spatial diffraction curves showing phase vs spatial frequency for (a) continuous and (b) discrete models. The arrows mark the largest possible angle of energy propagation for each model. An inversion of curvature (beyond $k_x d = \pm\pi/2$) leads to anomalous diffraction only in the discrete case.

 0031-9007/01/86(15)/3296(4)$15.00

analogy with temporal dispersion, the spatial broadening of the beam is related to $k_s'' = \partial^2 k_z/\partial k_x^2$. In homogeneous media, k_s'' is always negative, implying that diffraction in such media is equivalent to anomalous dispersion.

Let us now consider the spatial broadening of a beam in a *discrete* system, such as an infinite array of weakly coupled identical waveguides. In this system all the guides support the same optical mode, and energy can be exchanged between neighboring guides through the overlap of their modes. The optical coupled-mode set of equations for the electrical field in the nth waveguide is [4,5]

$$\frac{dE_n}{dz} = ik_{wg}E_n + iC(E_{n-1} + E_{n+1}) + i\gamma|E_n|^2 E_n \, . \tag{1}$$

In Eq. (1), k_{wg} is the propagation constant of the waveguide, and C is the coupling constant between adjacent waveguides, which is proportional to an overlap integral of the two modes of such waveguides. The last term describes the nonlinear Kerr effect, with a coefficient γ. When a single, or few, input guides are excited with low optical power, light spreads over more and more waveguides as it propagates through "discrete diffraction." Similar dynamical properties are shared by many other discrete systems in nature, e.g., molecular chains, crystal lattices or two- and three-dimensional photonic crystals [6–9].

In analogy with dispersion and continuous diffraction, discrete diffraction is best formulated in terms of plane wave excitations of the infinite array. The diffraction relation [10] can be deduced from the coupled-mode equation (1), which is the optical equivalent of the continuous model of tight binding of electrons in a one-dimensional atomic lattice [11]. As in solid-state physics, similar qualitative results can be derived from the Floquet-Bloch wave theory for a weak periodic potential [12]. The linear diffraction relation between k_z and k_x is $k_z = k_{wg} + 2C\cos(k_x d)$, where d is the distance between the waveguide centers [Fig. 1(b)]. The periodic diffraction relation reflects the fact that once a plane wave is tilted by an angle of λ/d, or integer multiples, adjacent waveguides are excited in phase, just as the excitation of a wave normal to the array. The periodic dispersion relation has a significant effect on diffraction. Now $k_s'' = -2Cd^2\cos(k_x d)$, and the diffraction sign can be controlled. In particular, k_s'' is positive (i.e., of the opposite sign to that normally experienced in nature) in the range $\pi/2 < |k_x d| \leq \pi$, where the diffraction is *anomalous*. Diffraction vanishes at the two points $k_x = \pm\pi/2d$. Clearly, the sign and value of diffraction can be chosen by launching light at a particular angle. The ability to control diffraction was recently shown in engineered periodical arrays of waveguides [10].

For nonlinear propagation, the implications are even more interesting. Dispersion always causes the spreading of light pulses, and diffraction broadens light beams, regardless of their sign. However, it is well known that a positive (focusing) Kerr nonlinearity may counterbalance and even cancel the effect of anomalous dispersion to generate a stable nondispersing bright temporal soliton. In the normal dispersion regime it is possible to launch dark solitons, which have the form of a stable dip in a uniform background of light [13].

Because of the unique sign of diffraction, dark *spatial* solitons have been generated only in materials with a slow negative nonlinearity [14]. Here we demonstrate that the condition necessary to observe the nonlinear consequences of anomalous diffraction can be created in an array of waveguides. When the light is injected normal to the input facet ($k_x d \sim 0$), the diffraction is normal and the array exhibits discrete self-focusing that leads eventually to the formation of a bright discrete soliton [5,15]. By slightly

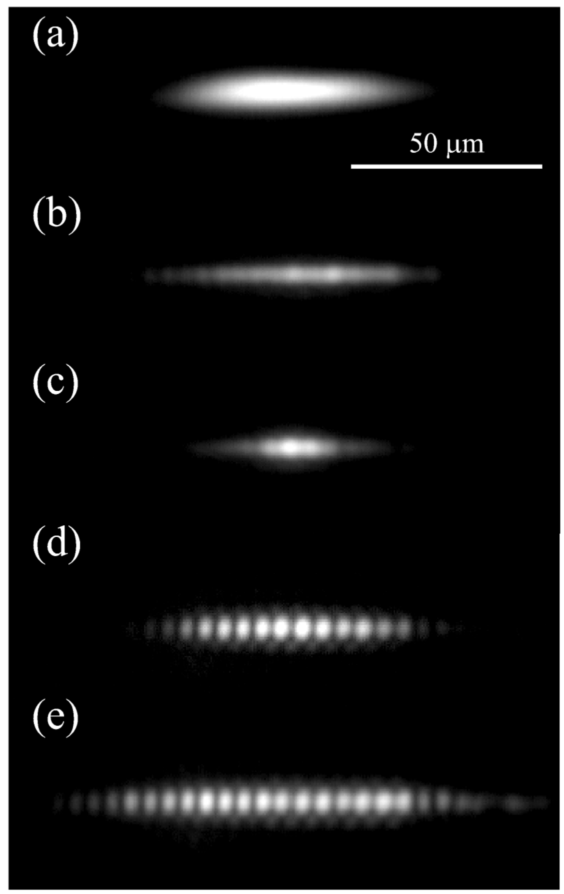

FIG. 2. Experimental results showing both nonlinear self-focusing and self-defocusing in an array of waveguides, for slightly different initial conditions. (a) The input beam, ~35 μm wide at FWHM. (b) Light distribution at the output facet for normal dispersion in the linear regime. The beam slightly broadens through discrete diffraction. (c) At high power ($I_{\text{peak}} \sim 150$ W), the field shrinks and evolves into a discrete bright soliton. (d) For an anomalous dispersion condition, when the beam is injected at an angle of 2.6° ± 0.4° inside the array, it broadens slightly as in (b). Note the dark lines between the optical modes resulting from the π-phase flips between adjacent waveguides. (e) When the power is increased ($I_{\text{peak}} \sim 100$ W), the distribution broadens significantly due to self-defocusing.

tilting the input beam, we can induce the phase shift between adjacent waveguides [16] that is required in order to generate anomalous diffraction and nonlinear discrete self-defocusing at higher powers. Under such conditions, an infinite beam with a phase flip across its center will evolve into a stable dark soliton, even in a medium with a positive Kerr nonlinearity, as proposed by Kivshar and co-workers [17,18].

The light source in the experiments was a mode-locked optical parametric oscillator emitting 100 fs pulses tuned to 1.53 μm, which is slightly below the half-bandgap energy of GaAs. The nonlinearity of AlGaAs in this wavelength range is primarily due to instantaneous nonresonant electronic interaction, and it can be described well as a pure positive Kerr nonlinearity. The experimental setup is similar to the one described in Refs. [15,16].

The first set of results, presented in Fig. 2, depicts the nonlinear behavior in regions of normal and anomalous diffraction. The sample was a 6-mm-long array (corresponding to about three coupling lengths) consisting of 61 rib waveguides, 2.5 μm wide, uniformly spaced by 2.5 μm and etched 1.6 μm deep on top of a slab waveguide [15]. Figure 2(a) shows the input beam, initially 35 μm wide, which is injected into the array. Figures 2(b)–2(e) display images of the light distribution at the output facet. In particular, Figs. 2(b) and 2(c) are for excitation perpendicular to the array's input facet ($k_x d \sim 0$), where diffraction is normal. Figure 2(b) shows the expansion of the beam at low power, while Fig. 2(c) illustrates the effect of self-focusing resulting in the formation of a bright discrete soliton [15]. The conditions of anomalous diffraction were achieved by tilting the input beam by about 3°. At this input condition, light in adjacent waveguides is out of phase, as confirmed by the pronounced dark dips between adjacent waveguide modes. At low power, the beam still broadens [Fig. 2(d)]. When the light intensity is increased [Fig. 2(e)], the output field does not focus but rather spreads and becomes significantly wider, indicating nonlinear self-defocusing even though the nonlinearity is positive.

We have compared our experimental results with the numerical solutions [19] of the coupled mode equation (1). In Fig. 3 we show measured horizontal cross-sections through the four experimental patterns of Figs. 2(b)–2(e), which are represented by the solid lines in Figs. 3(a)–3(d). The simulation results are given by the solid circles in Fig. 3. Each circle represents the intensity $|E_n|^2$ in the corresponding waveguide. These simulated values

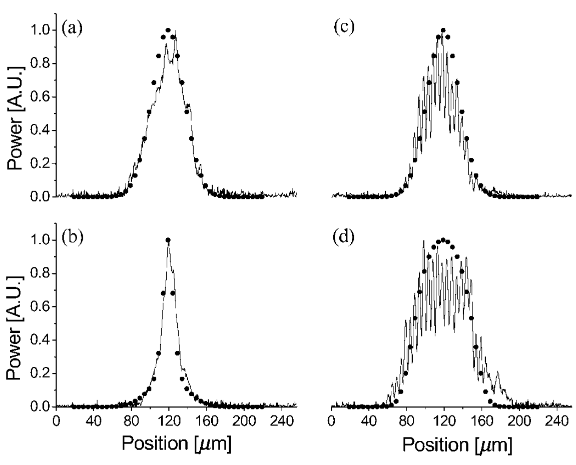

FIG. 3. Comparison between cross sections of the experimental results of Fig. 2 (continuous line) and numerical solutions of coupled-mode theory (solid circles, each represents the power in a single waveguide). (a),(b) Normal discrete diffraction condition, low and high power, respectively. (c),(d) Anomalous diffraction condition, low and high power, respectively. Note the difference between nonlinear focusing (b) and defocusing (d).

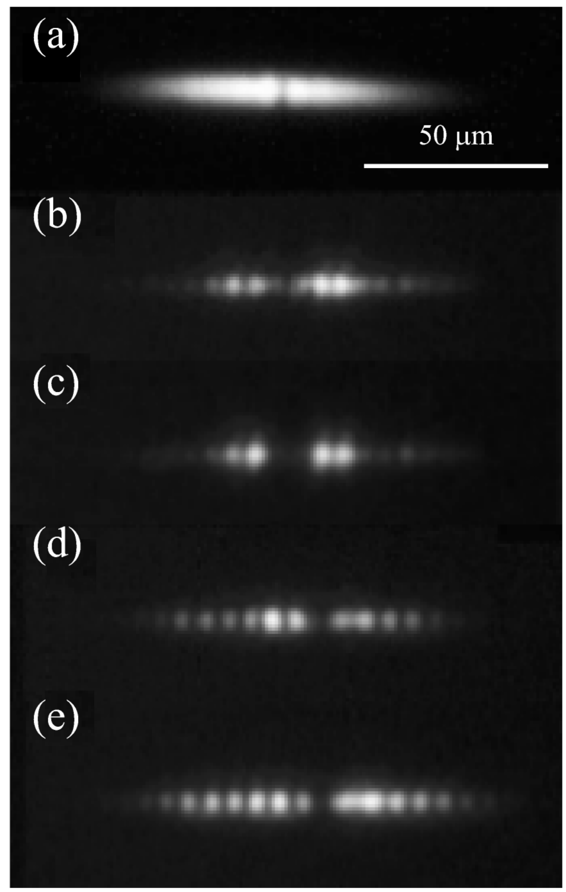

FIG. 4. Generation of a dark discrete solitary wave in the case of anomalous diffraction. (a) The input profile, ~40 μm wide at FWHM. (b) For normal diffraction at low power, a notch is visible in the output profile. The beam evolves into two repulsive bright solitons when the intensity is increased [(c) $I_{\text{peak}} \sim 250$ W]. For anomalous diffraction (beam tilt = 2.0° ± 0.4° in this array), the "dark" notch initially present in the output profile [(d) linear case] slightly narrows and becomes more marked when the power is increased [(e) $I_{\text{peak}} \sim 250$ W]. As a result of anomalous diffraction, the dark localization is self-sustained in a defocusing bright background, and does not disappear when the beam broadens nonlinearly.

correspond quite well with the peaks of the intensity distribution corresponding to the individual waveguides.

Subsequently, we tested a sample consisting of a 4-mm-long array (about two coupling lengths) of 61 waveguides, 3 μm wide and separated by the same distance. By adding a suitable phase mask just before the input, we created a π-phase shift in the center of the beam, corresponding to a sharp dark strip [Fig. 4(a)]. For normal diffraction, the dark notch was still observed at low powers in the output profile [Fig. 4(b)], but the beam evolved into two discrete bright solitons when the power was increased [Fig. 4(c)]. The same experiment was subsequently repeated in conditions of anomalous diffraction. The dark notch was still visible in the output profile of the array, both at low [Fig. 4(d)] and at high [Fig. 4(e)] powers, when it slightly narrows but becomes more marked. However, we note that self-defocusing causes an almost symmetric spreading of the beam, while remarkably preserving the narrow central dark region. Even if the strict conditions to observe dark solitons were not met, as higher powers would be required to induce nonlinear behavior with a significantly broader beam, the characteristic behavior of a dark excitation for the two diffraction regimes is clearly seen in the figures.

In conclusion, we investigated the nonlinear diffractive properties of a waveguide array. When the beam was injected normal to the input facet, we observed nonlinear self-focusing and the formation of a bright spatial soliton. However, by a slight variation of the input angle, we achieved the condition of anomalous diffraction and observed self-defocusing. Taking advantage of these features, we used a phase mask to generate a dark solitary wave in the presence of a positive, ultrafast Kerr nonlinearity. We believe that these results could have important consequences in the fabrication of optoelectronic circuits, where nonlinear self-focusing poses a serious limitation on the performances of many devices. The properties observed are quite general, and can be used to suggest novel behavior in discrete systems of a rather different nature. In particular, it is possible to imagine photonic crystal structures in which diffraction strongly depends on the propagation direction, to the point that two different orthogonal directions could support nonlinear self-focusing and defocusing simultaneously.

The authors thank D. Modotto and U. Peschel for different contributions to this work. We also acknowledge the EPSRC in the United Kingdom and the Ministry of Science and Technology in Israel for financial support to this project.

*Also with the Department of Electronics and Electrical Engineering, University of Glasgow, Glasgow, Scotland, G12 8QQ.

[1] A. Hasegawa and F. Tappert, Appl. Phys. Lett. **23**, 142 (1973); **23**, 171 (1973).
[2] L. F. Mollenauer, R. H. Stolen, and J. P. Gordon, Phys. Rev. Lett. **45**, 1095 (1980).
[3] A. M. Weiner, J. P. Heritage, R. J. Hawkins, R. N. Thurston, E. M. Kirschner, D. E. Leaird, and W. Tomlinson, Phys. Rev. Lett. **61**, 2445 (1988).
[4] S. Somekh, E. Garmire, A. Yariv, H. L. Garvin, and R. G. Hunsperger, Appl. Phys. Lett. **22**, 46 (1973).
[5] D. N. Christodoulides and R. I. Joseph, Opt. Lett. **13**, 794 (1988).
[6] W. P. Su, J. R. Schrieffer, and A. J. Heeger, Phys. Rev. Lett. **42**, 1698 (1979).
[7] P. Marquié, J. M. Bilbault, and M. Remoissenet, Phys. Rev. E **51**, 6127 (1995).
[8] B. Denardo, B. Galvin, A. Greenfield, A. Larraza, S. Putterman, and W. Wright, Phys. Rev. Lett. **68**, 1730 (1992).
[9] H. Kosaka, T. Kawashima, A. Tomita, M. Notomi, T. Tamakura, T. Sato, and S. Kawakami, Appl. Phys. Lett. **74**, 1212 (1999).
[10] H. S. Eisenberg, Y. Silberberg, R. Morandotti, and J. S. Aitchison, Phys. Rev. Lett. **85**, 1863 (2000).
[11] N. W. Ashcroft and N. D. Mermin, *Solid State Physics* (Holt, Rinehart, and Winston, New York, 1976), p. 182.
[12] P. St. J. Russell, Appl. Phys. B **39**, 231 (1986).
[13] While instantaneous electronic nonlinearities are positive (refractive index increases with light intensity), other mechanisms could lead to negative nonlinearities, which are usually slow. In homogeneous negative nonlinear media, only dark spatial solitons are possible [14].
[14] G. A. Swartzlander, Jr., D. R. Andersen, J. J. Regan, H. Yin, and A. E. Kaplan, Phys. Rev. Lett. **66**, 1583 (1991).
[15] H. S. Eisenberg, Y. Silberberg, R. Morandotti, A. R. Boyd, and J. S. Aitchison, Phys. Rev. Lett. **81**, 3383 (1998).
[16] R. Morandotti, U. Peschel, J. S. Aitchison, H. S. Eisenberg, and Y. Silberberg, Phys. Rev. Lett. **83**, 2726 (1999).
[17] Y. S. Kivshar, W. Królikowski, and O. A. Chubykalo, Phys. Rev. E **50**, 5020 (1994).
[18] A. N. Slavin, Y. S. Kivshar, E. A. Ostrovskaya, and H. Benner, Phys. Rev. Lett. **82**, 2583 (1999).
[19] Numerical simulations were performed using "*FreeBPM*" software (http://www.weizmann.ac.il/~feisen/freebpm).